International Review of Mechanical Engineering (I.RE.M.E.), Vol. 17, N. 12
ISSN 1970 - 8734 December 2023

Roll and Pitch Motion Control Using Active Suspension Under Combined Steering and Braking Inputs

Adam Puah Leong Zhin[1], Amrik Singh Phuman Singh[1, 2],
Khairil Anwar Abu Kassim[3], Fauzi Ahmad[1, 2], Mohd Azman Abdullah[1, 2]

Abstract – *Excessive vertical, roll, and pitch motions of the vehicle can cause discomfort for the driver and passengers. Mitigation of such motions can be done using active suspensions. In this paper, proportional-derivative controllers are used to reduce the vertical, roll, and pitch motions by using a 10 degree-of-freedom vehicle model. The vehicle model is verified by using CarSim for a double lane change maneuver. The verification results have showed that the vehicle model used in this study can emulate the motion of the vehicle model in CarSim. The proportional-derivative controllers are used to calculate the desired vehicle vertical force, roll moment, and pitch moment. These desired force and moments are converted into active suspension force inputs by using decoupling transformation. When the vehicle is given sine steer wave and braking torque inputs, the results have showed that the controllers can reduce the vertical, roll, and pitch motions considerably.*

Keywords*: Active Suspension, Pitch, Roll, Vehicle Control System, Vehicle Dynamics*

Nomenclature

a_x	Vehicle longitudinal acceleration
a_y	Vehicle lateral acceleration
a_z	Vehicle vertical acceleration
c_s	Suspension damping coefficient
C_α	Lateral tire stiffness
C_σ	Longitudinal tire stiffness
e_p	Vehicle roll angle error
e_q	Vehicle pitch angle error
e_z	Vehicle vertical displacement error
F_{ci}	Total suspension force
F_{ui}	Active suspension force
F_{xi}	Longitudinal tire force
F_{yi}	Lateral tire force
F_{zi}	Vertical tire force
F_{zd}	Desired vertical vehicle force
h_g	Height of vehicle's center of gravity from ground
i	Subscript for indicating the position of the tire (i = *fl*, *fr*, *rl*, and *rr* for front left, front right, rear left, and rear right, respectively)
I_w	Moment of inertia of the wheel
I_x	Roll moment of inertia of the vehicle
I_y	Pitch moment of inertia of the vehicle
I_z	Yaw moment of inertia of the vehicle
k_{ax}	Proportional gain for vehicle longitudinal acceleration
k_{ay}	Proportional gain for vehicle lateral acceleration
k_{az}	Proportional gain for vehicle vertical acceleration
k_{dp}	Derivative gain for vehicle roll angle error
k_{dq}	Derivative gain for vehicle pitch angle error
k_{dz}	Derivative gain for vehicle vertical displacement error
k_{pp}	Proportional gain for vehicle roll angle error
k_{pq}	Proportional gain for vehicle pitch angle error
k_{pz}	Proportional gain for vehicle vertical displacement error
k_s	Suspension spring stiffness
L_f	Distance from front axle to the vehicle's center of gravity
L_r	Distance from rear axle to the vehicle's center of gravity
L_w	Track width
m	Mass of vehicle
M_{pd}	Desired roll moment
M_{qd}	Desired pitch moment
p	Roll rate of the vehicle
q	Pitch rate of the vehicle
r	Yaw rate of the vehicle
R_w	Tire radius
s	Slip ratio
T_i	Wheel torque
v_x	Longitudinal velocity of vehicle
v_y	Lateral velocity of vehicle
v_z	Vertical velocity of vehicle
z_{ba}	Actual vehicle vertical displacement
z_{bd}	Desired vehicle vertical displacement
z_i	Vertical displacement of each corner of the vehicle
α	Slip angle
δ	Front steering angle
θ_a	Actual vehicle pitch angle
θ_d	Desired vehicle pitch angle
μ	Tire-road friction coefficient
ϕ_a	Actual vehicle roll angle

 https://doi.org/10.15866/ireme.v17i12.22604

ϕ_d Desired vehicle roll angle
Ω Angular velocity of the tire

I. Introduction

The safety of a vehicle is important to protect the driver and passengers in it. Hence, studies on vehicle safety systems such as collision avoidance [1], [2], rollover prevention [3]-[5], and vehicle stability systems, are imperative to improve the safety of a vehicle. Whenever a vehicle is given steering angle or wheel torque input, the vehicle will experience a roll or pitch moment, respectively. For the passengers and the driver, they will feel that their bodies are moving sideways, or forward or backward, respectively. Repetitive of such motions in different directions would cause discomfort or nausea to both the passengers and driver. A suspension system is required to reduce such motions, improving the comfort of the passenger and driver. The suspension system can be divided into passive, semi-active, and active suspension systems. A passive suspension system consists of four sets of springs and dampers at each corner of the vehicle. A semi-active suspension system works by controlling the damping coefficient of the damping fluid in the dampers.

An active suspension system is comprised of an electronically controlled actuator at each corner of the vehicle. This paper has focused on evaluating the performance of the active suspension control system to reduce the vertical, roll, and pitch motions of the vehicle.

Many studies have used semi-active suspension control to reduce the roll [6], [7] and pitch [7], [8] motions of the vehicle. Likewise, there are also studies on active suspension control to reduce the roll [9], [10] and pitch [11], [12] motions of the vehicle. The other methods to reduce the roll motion of the vehicle are anti-roll bar control [13] while braking control [14], [15] can be used to reduce the pitch motion of the vehicle. Some studies have used semi-active suspension control [4], anti-roll bar control [16], Direct Yaw-moment Control (DYC) [17]-[19], active steering control [3], [20], [21], and combination of acting steering control and DYC [5], [22], [23] for rollover prevention. Besides that, a rollover prevention method was proposed by using a gyroscopic device that applies counter roll moment to the vehicle body [24]. Ochi et al. [25] have proposed the usage of anti-dive force to control the roll angle by manipulating the longitudinal tire forces generated by each electric in-wheel motor. In literature, various control approaches are used to reduce the roll motion of the vehicle. The controllers compute active suspension forces, braking torque, or steering angle in such a way that the roll angle is reduced. In [4], Yoon et al. have developed a Sliding Mode Controller (SMC) to compute the desired roll moment based on the sliding surface, which is defined as the weighted function of roll angle and roll rate. This study has been extended with the addition of active steering control in [5]. For [9], a Fuzzy Logic Controller (FLC) has been used for feedback and feedforward control.

The feedforward FLC computes the counter roll moment based on the steering angle and longitudinal vehicle velocity. The feedback FLC computes a counter roll moment based on the roll angle error and error rate.

The sum of the counter roll moments generated by the two FLCs is the desired total counter roll moment. Kadir et al. [10] have used FLC to compute the vehicle body vertical force and counter roll moment to suppress the vertical displacement and roll angle, which are then distributed to four pneumatic suspensions to be realized.

Cho et al. [7] have proposed an integrated control scheme that uses proportional-derivative controllers to calculate the desired roll, pitch, and yaw moments. These desired moments are distributed to the semi-active suspension system by using two optimization algorithms that calculate the output damping force and final damping, respectively, and a control value compensation module that considers the actuator limitations. Vu et al. [13] tackle the roll stability problem of a heavy vehicle by using a Linear Quadratic Regulator (LQR) to control the anti-roll bar while considering the input control limitation of the hydraulic actuator. In [18], a feedforward DYC has been used in conjunction with tire force distribution control in order to improve the roll stability of the vehicle.

Similarly, the pitch motion of the vehicle has been improved by using different controllers. In [12], an adaptive PID controller for an active suspension system has been used to reduce the pitch angle and pitch rate. Sato and Fujimoto [14] have proposed state feedback control for braking torque to reduce the pitching motion. The slip ratio is estimated to calculate the braking torque by using a Proportional-Integral controller (PI).

Tavernini et al. [15] have computed the optimal braking distribution for minimum pitch angle by using Model Predictive Control (MPC).

In this paper, the vertical, roll, and pitch motions of a 10 Degree Of Freedom (DOF) vehicle model under combined steering and braking torque is controlled using three Proportional-Derivative (PD) controllers with the addition of the product of the accelerations in respective axis and gains. The effectiveness of the controllers is evaluated by giving single sine wave steer and braking torque.

The remainder of this paper is organized as follows. Section II describes the vehicle model used in the simulations. Section III presents the controller used for the active suspension system and describes how the force and moments calculated by the controller are distributed to the active suspension actuator. Section IV shows the results of two verification tests and the combination of sine wave steering and braking tests for two different tire-road friction coefficient. Section V presents the conclusion of the study.

II. Vehicle System Model

A vehicle model represents a set of equations that describe the motions of a vehicle. The vehicle model that is used in this paper is shown in Fig. 1.

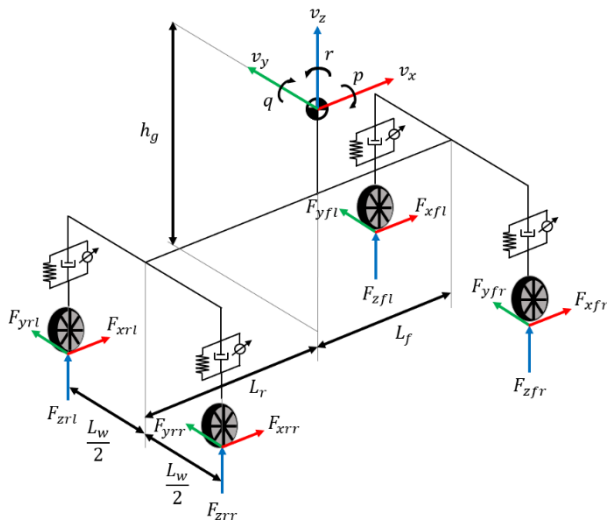

Fig. 1. Vehicle dynamics model

The vehicle model has 10 Degree-Of-Freedom (DOF): 6 DOF at the vehicle's Center of Gravity (CG) and 4 DOF for the wheel spin dynamics. It can be noted that the vehicle model used in this study is capable of four-Wheel Independent Driving or Braking (4WIDB) and two-Wheel Steering (2WS) for the front wheels.

II.1. 10 DOF Vehicle Model

The 6 DOF at the vehicle's CG comprised of three translational and three rotational motions of the vehicle.

The three translational motions are the longitudinal, lateral, and vertical motions at the vehicle's CG, which can be represented by the following equations, respectively:

$$\begin{aligned} m(\dot{v}_x - v_y r + v_z q) &= (F_{xfl} + F_{xfr})\cos\delta \\ &\quad - (F_{yfl} + F_{yfr})\sin\delta + F_{xrl} + F_{xrr} \end{aligned} \tag{1}$$

$$\begin{aligned} m(\dot{v}_y + v_x r - v_z p) &= (F_{xfl} + F_{xfr})\sin\delta \\ &\quad + (F_{yfl} + F_{yfr})\cos\delta + F_{yrl} \\ &\quad + F_{yrr} \end{aligned} \tag{2}$$

$$m(\dot{v}_z - v_x q + v_y p) = F_{cfl} + F_{cfr} + F_{crl} + F_{crr} \tag{3}$$

where v_x, v_y, and v_z are the longitudinal, the lateral, and the vertical velocities at the vehicle's CG, respectively. The roll, pitch, and yaw rates at the vehicle's CG are represented by the symbols p, q, and r, respectively. m denotes the total mass of the vehicle while δ is the steering angle for the two front wheels. F_{xi} and F_{yi} denote the longitudinal and lateral tire forces, respectively while F_{ci} denotes the suspension forces acting on the vehicle. The subscript i = *fl*, *fr*, *rl*, and *rr* represent the front left, the front right, the rear left, and the rear right tires, respectively.

The three rotational motions are roll, pitch, and yaw, which can be described by the following equations, respectively:

$$\begin{aligned} I_x\dot{p} = h_g[&(F_{xfl} + F_{xfr})\sin\delta + (F_{yfl} + F_{yfr})\cos\delta \\ &+ F_{yrl} + F_{yrr}] \\ &+ \frac{L_w}{2}(F_{cfl} - F_{cfr} + F_{crl} - F_{crr}) \end{aligned} \tag{4}$$

$$\begin{aligned} I_y\dot{q} = h_g[&(F_{yfl} + F_{yfr})\sin\delta \\ &- (F_{xfl} + F_{xfr})\cos\delta - F_{xrl} \\ &- F_{xrr}] - L_f(F_{cfl} + F_{cfr}) \\ &+ L_r(F_{crl} + F_{crr}) \end{aligned} \tag{5}$$

$$\begin{aligned} I_z\dot{r} = \frac{L_w}{2}[&(-F_{xfl} + F_{xfr})\cos\delta - F_{xrl} + F_{xrr} \\ &+ (F_{yfl} - F_{yfr})\sin\delta] \\ &- L_r(F_{yrl} + F_{yrr}) \\ &+ L_f[(F_{xfl} + F_{xfr})\sin\delta \\ &+ (F_{yfl} + F_{yfr})\cos\delta] \end{aligned} \tag{6}$$

where h_g is the height of the vehicle's CG from the ground.

L_f and L_r are the distances of the front and rear axles from the vehicle's CG, respectively. L_w denotes the distance between the left and right tires, in which both tires are equally spaced from the vehicle's CG. The roll, pitch, and yaw moments of inertia of the vehicle are denoted by I_x, I_y, and I_z, respectively.

The wheel spin dynamics can be described by:

$$I_w\dot{\Omega}_i = T_i - R_w F_{xi} \tag{7}$$

where I_w is the moment of inertia of the wheel, Ω is the angular velocity of the tire, T is the wheel torque, and R_w is the tire radius.

II.2. Suspension System

The suspension system is comprised of four sets of springs, dampers, and active suspension actuators. The suspension forces produced by all the components can be represented by:

$$F_{ci} = -k_{si}z_i - c_{si}\dot{z}_i + F_{ui} \tag{8}$$

where k_s and c_s are the suspension spring stiffness and damping coefficient, respectively. The vertical displacement of each end of the axles is denoted by the symbol z. F_u is the force produced by the active suspension actuator.

II.3. Tire Model

The tire model for the vehicle model is Dugoff's tire model. The equations provided by [26] that describe the longitudinal and lateral tire forces F_x and F_y, respectively, are:

$$F_x = C_\sigma \frac{s}{1+s} f(\lambda) \tag{9}$$

$$F_y = -C_\alpha \frac{\tan\alpha}{1+s} f(\lambda) \tag{10}$$

where C_σ and C_α are the longitudinal and lateral tire stiffnesses, respectively. s and α are the longitudinal slip ratio and slip angle, respectively. The function $f(\lambda)$ is defined as:

$$f(\lambda) = \begin{cases} (2-\lambda)\lambda & \text{if } \lambda < 1 \\ 1 & \text{if } \lambda \geq 1 \end{cases} \tag{11}$$

where the variable λ is given as:

$$\lambda = \frac{\mu F_z (1+s)}{2\sqrt{(C_\sigma s)^2 + (C_\alpha \tan\alpha)^2}} \tag{12}$$

where μ is the tire-road friction coefficient and F_z is the vertical tire force.

III. Active Suspension Control System

In this section, the active suspension controller and decoupling transformation are described. The active suspension controllers calculate the desired vehicle vertical force, roll moment, and pitch moment to reduce the vertical, roll, and pitch motions [28]-[31]. The decoupling transformation translates these force and moments into active suspension forces for each corner of the vehicle to reduce errors. The block diagram shown in Fig. 2 illustrates the interaction between the active suspension controller, decoupling transformation, and vehicle dynamics model.

III.1. Active Suspension Controller

During acceleration or deceleration, a vehicle will experience a pitching moment. When a vehicle is turning, the vehicle will experience a roll moment. In both cases, the vehicle will also experience heave motion. An active suspension controller is needed to reduce the pitch, roll, and heave motions of the vehicle, ideally eliminating them.

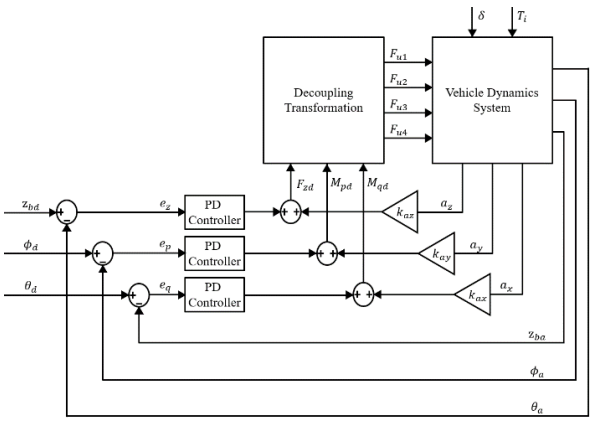

Fig. 2. Block diagram of the active suspension

In this study, three Proportional-Derivative (PD) controllers in addition to their respective products of gain and acceleration are used to determine the desired vertical vehicle force, F_{zd} and desired roll and pitch moments M_{pd} and M_{qd}, to reduce the heave, roll, and pitch motions generated from acceleration or deceleration and turning.

The equations for the PD controllers are given as follows:

$$F_{zd} = k_{pz} e_z + k_{dz} \dot{e}_z + k_{az} a_z \tag{13}$$

$$M_{pd} = k_{pp} e_p + k_{dp} \dot{e}_p + k_{ay} a_y \tag{14}$$

$$M_{qd} = k_{pq} e_q + k_{dq} \dot{e}_q + k_{ax} a_x \tag{15}$$

where k_{ax}, k_{ay}, and k_{az} are the proportional gains for the longitudinal, lateral, and vertical accelerations, a_x, a_y, and a_z, respectively. k_{pz}, $k_{p\varphi}$, and $k_{p\theta}$ are the proportional gains for the vertical, roll, and pitch errors, e_z, e_φ, and e_θ, respectively. The derivative gains for the error rates for vertical, roll, and pitch are denoted by k_{dz}, $k_{d\varphi}$, and $k_{d\theta}$, respectively.

The first and second terms in Equations (13) to (15) represent the PD controllers. The third terms represent the product of the gain and the acceleration in each axis. The errors are defined as:

$$e_z = z_{bd} - z_{ba} \tag{16}$$

$$e_p = \phi_d - \phi_a \tag{17}$$

$$e_q = \theta_d - \theta_a \tag{18}$$

where z_{bd}, ϕ_d, and θ_d are the desired vehicle vertical displacement, roll angle, and pitch angle, respectively.

Ideally, it is desired to have zero vertical displacement, roll angle, and pitch angle on the vehicle, thus these variables are set to zero. z_{ba}, ϕ_a, and θ_a are the actual vertical displacement, roll angle, and pitch angle of the vehicle, respectively.

III.2. Decoupling Transformation

By using decoupling transformation provided by [27], the desired vertical vehicle force and desired pitch and roll moments can be converted into the active suspension forces. The active suspension forces for each corner of the vehicle by using the decoupling transformation are given as:

$$F_{ufl} = \frac{L_r F_{zd}}{2(L_f + L_r)} - \frac{M_{qd}}{2(L_f + L_r)} + \frac{M_{pd}}{2L_w} \tag{19}$$

$$F_{ufr} = \frac{L_r F_{zd}}{2(L_f + L_r)} - \frac{M_{qd}}{2(L_f + L_r)} - \frac{M_{pd}}{2L_w} \tag{20}$$

$$F_{url} = \frac{L_f F_{zd}}{2(L_f + L_r)} + \frac{M_{qd}}{2(L_f + L_r)} + \frac{M_{pd}}{2L_w} \tag{21}$$

$$F_{urr} = \frac{L_f F_{zd}}{2(L_f + L_r)} + \frac{M_{qd}}{2(L_f + L_r)} - \frac{M_{pd}}{2L_w} \quad (22)$$

IV. Numerical Examples

In this section, simulations are conducted to verify the vehicle model and to evaluate the performance of the proposed controller. The two simulations performed to verify the vehicle model are for the double lane change and step steering input tests. The results of the simulations are compared with CarSim, which is a vehicle dynamics simulation software. Additional two simulations are performed to evaluate the performance of the controller in reducing the vertical displacement, vertical velocity, roll angle, roll rate, pitch angle, and pitch rate errors.

IV.1. Verification of Vehicle Model

In this subsection, two verification results for the 10 DOF vehicle model are presented. For the verification purpose, CarSim, which is a vehicle dynamics software, is used.

The first verification test is a double lane change test with an initial velocity of 90 km/h. The front steering angle from CarSim is used as the input for the Simulink model. The second verification test is a step steering input test with a constant vehicle velocity of 50 km/h. A front steering angle of 60 deg is given at 1 s and maintained throughout the remaining duration of the simulation.

The comparisons between the responses for the lateral acceleration, yaw rate, roll angle, roll rate, front slip angle, and rear slip angle of the CarSim and Simulink models for double lane change maneuver are shown in Fig. 3 to Fig. 8, respectively. For Fig. 3 to Fig. 6, the red solid line represents the response of the Simulink model while the blue dash-dotted line represents the response of the CarSim model.

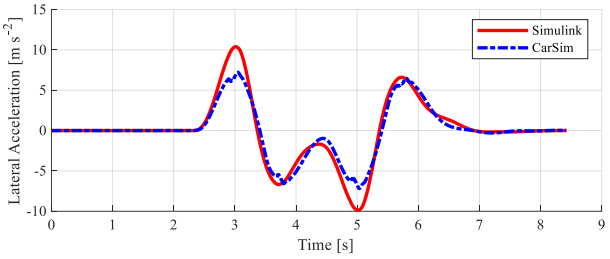

Fig. 3. Lateral acceleration for double lane change maneuver

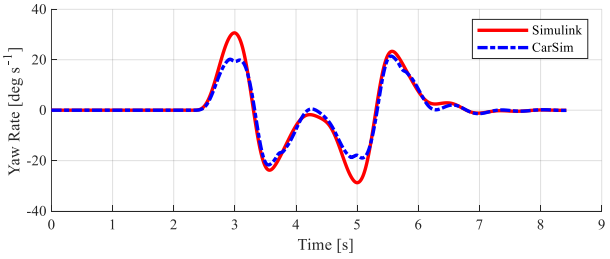

Fig. 4. Yaw rate for double lane change maneuver

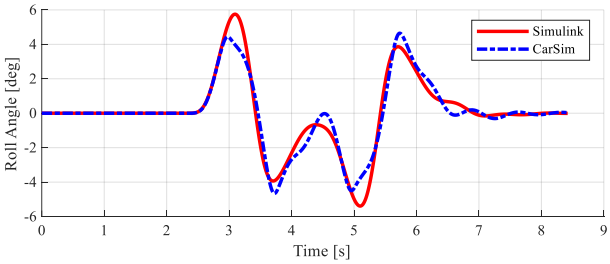

Fig. 5. Roll angle for double lane change maneuver

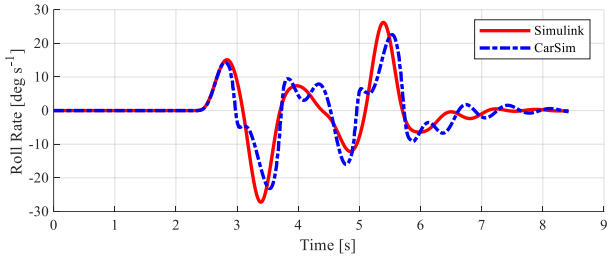

Fig. 6. Roll rate for double lane change maneuver

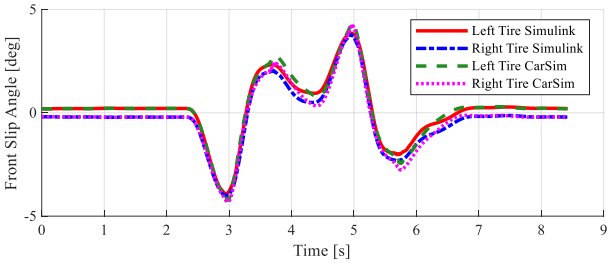

Fig. 7. Front slip angle for double lane change maneuver

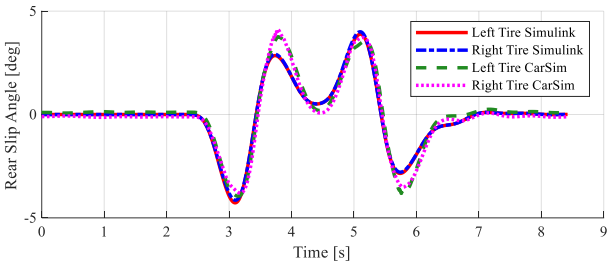

Fig. 8. Rear slip angle for double lane change maneuver

For Fig. 7 and Fig. 8, the red solid and the blue dash-dotted line represent the left and right tire of the Simulink model, respectively while the green dashed and the magenta dotted line represent the left and right tire of the CarSim model, respectively. Based on Fig. 3 to Fig. 8, it can be noted that the Simulink model could reproduce the responses that are generated by the CarSim model with acceptable deviations. The absolute values of the lateral acceleration and yaw rate of the Simulink model are larger than that of the CarSim model as shown in Fig. 3 and Fig. 4, respectively. The roll angle and roll rate of the Simulink model give higher absolute values than the CarSim model as shown in Fig. 5 and Fig. 6. On top of that, the roll angle and the roll rate are also roughly following the curves of the CarSim model as compared to the lateral acceleration and yaw rate.

The front and rear slip angles of the Simulink model could also follow closely with the CarSim model in Fig. 7 and Fig. 8, respectively. However, the rear slip angle of the Simulink model does not follow the CarSim model at approximately time t = 3.75, 4.50 and 5.75 s.

For step steering input maneuver, the Simulink and CarSim models are compared for lateral acceleration, yaw rate, roll angle, roll rate, front slip angle, and rear slip angle in Fig. 9 to Fig. 14, respectively. The red solid line represents the response of the Simulink model while the blue dash-dotted line represents the response of the CarSim model for Fig. 9 to Fig. 12. The red solid and the blue dash-dotted lines represent the left and right tires of the Simulink model, respectively while the green dashed and the magenta dotted lines represent the left and the right tire of the CarSim model, respectively for Fig. 13 and Fig. 14.

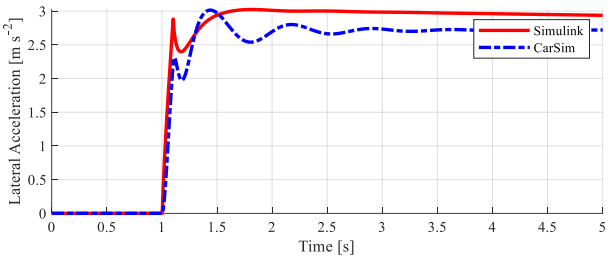

Fig. 9. Lateral acceleration for step steering input maneuver

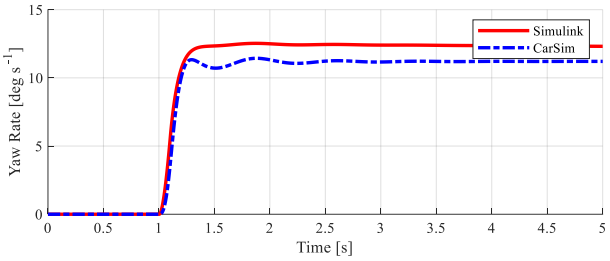

Fig. 10. Yaw rate for step steering input maneuver

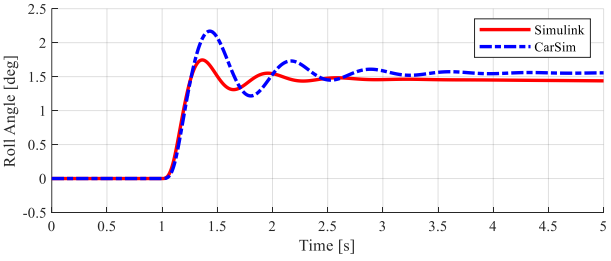

Fig. 11. Roll angle for step steering input maneuver

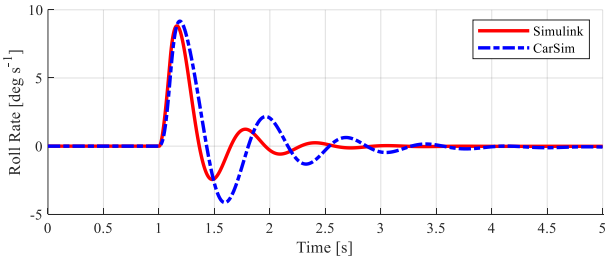

Fig. 12. Roll rate for step steering input maneuver

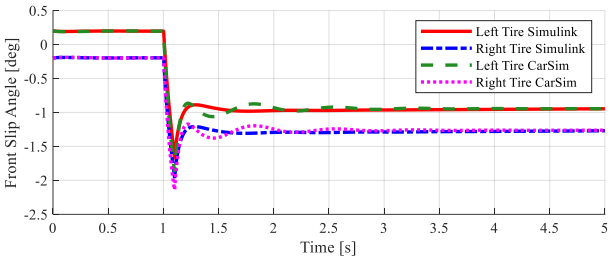

Fig. 13. Front slip angle for step steering input maneuver

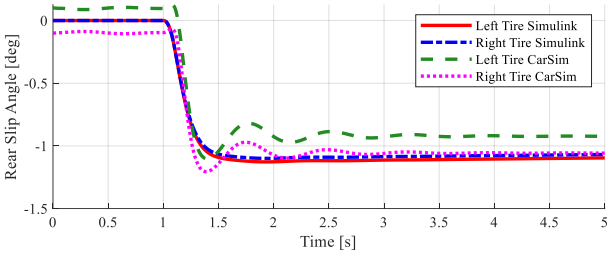

Fig. 14. Rear slip angle for step steering input maneuver

Based on Fig. 9 to Fig. 12, the Simulink model manages to follow the lateral acceleration, yaw rate, roll angle, and roll rate from the CarSim model closely when the steering input was given at 1 s. However, beyond 2 s, the lateral acceleration and the yaw rate from the Simulink model do not follow the CarSim model. Instead, the final values of the lateral acceleration and yaw rate of the Simulink model are higher than the CarSim model.

The roll angle of the Simulink model does not follow the CarSim model after 2 s and the final value of the Simulink model is lower than the CarSim model as shown in Fig. 11. The roll rate of the Simulink model does not follow the CarSim model after 2 s, but the final value of the roll rate of the Simulink model is approximately equal to the CarSim model in Fig. 12. The front slip angle of the Simulink model can follow closely with the CarSim model as shown in Fig. 13 while the rear slip angle of the Simulink model has a larger absolute value than the CarSim model as shown in Fig. 14.

IV.2. Effects of Controller

In this subsection, the performance of the active suspension control system in reducing the vertical, roll, and pitch motions are evaluated for two different tire-road friction coefficients. In both simulations, the front wheel steer angle and braking torque are given as inputs to the vehicle at time t = 0.5 s. The inputs for the steer angle and braking torque are shown in Fig. 15 and Fig. 16, respectively. The steer angle given to the vehicle is a single sine wave steer, which starts at 0.5 s and ends at 2.5 s with an amplitude of 3 deg. The braking torques for the front and rear wheels T_f and T_r are 350 Nm and 150 Nm, respectively. By using these inputs, two simulations are conducted and the vertical displacement, vertical velocity, roll angle, roll rate, pitch angle, and pitch rate of the vehicle are shown in Fig. 17 to Fig. 22, respectively.

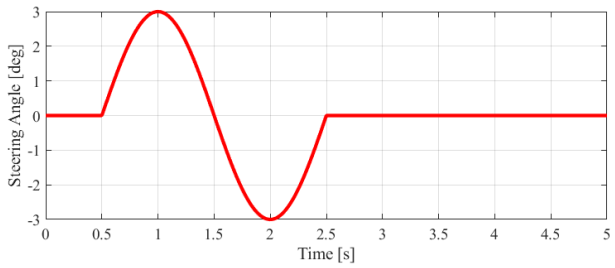

Fig. 15. Sine wave steer input

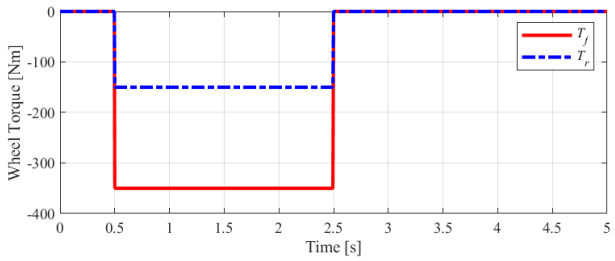

Fig. 16. Braking torque inputs for front and rear wheels

Based on Figs. 17(a) and (b), the vertical displacement of the vehicle oscillates upwards and downwards from its original position for μ = 0.9 and 0.5 without the controller.

With the controller, the amplitude of the oscillation for μ = 0.9 and 0.5 is reduced. The vertical velocity of the vehicle is also reduced for μ = 0.9 and 0.5 as shown in Figs. 18(a) and (b). Figs. 19(a) and (b) and Figs. 20(a) and (b) show that the vehicle model with the controller achieves lower maximum absolute values of the roll angle and roll rate of the vehicle compared to that of the vehicle without controller for μ = 0.9 and 0.5. For μ = 0.9, the maximum absolute values of the roll angle without and with controller are 3.34 and 1.32 deg, respectively while the maximum absolute values of roll angle without and with controller are 2.01 and 0.80 deg, respectively, when μ = 0.5.

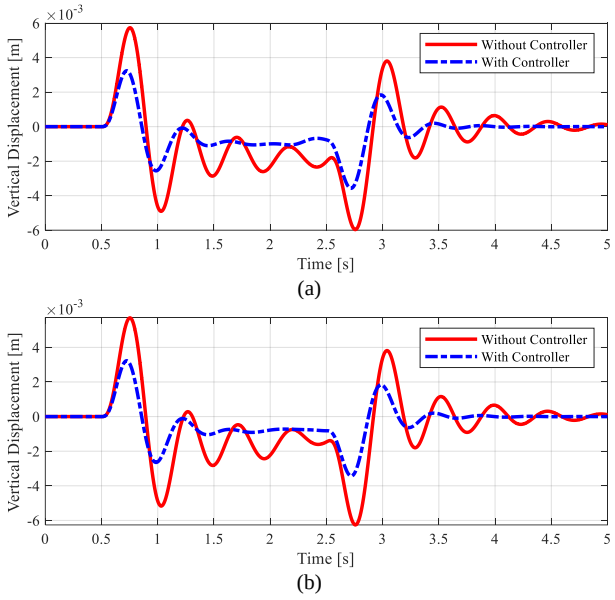

Figs. 17. Vertical displacement of vehicle for (a) μ = 0.9 (b) μ = 0.5

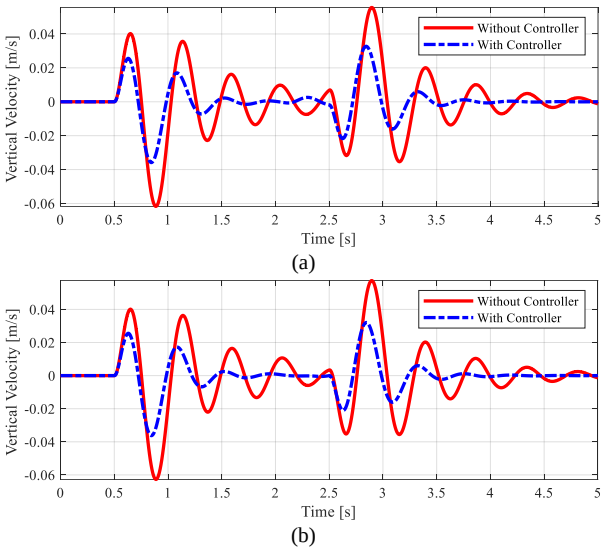

Figs. 18. Vertical velocity of vehicle for (a) μ = 0.9 (b) μ = 0.5

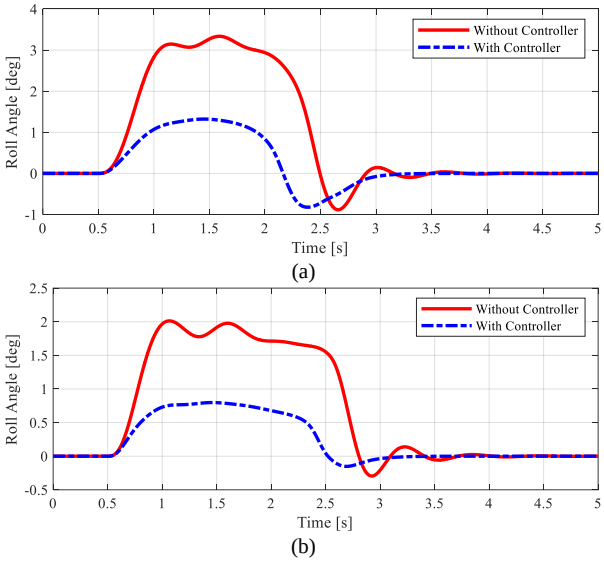

Figs. 19. Roll angle of vehicle for (a) μ = 0.9 (b) μ = 0.5

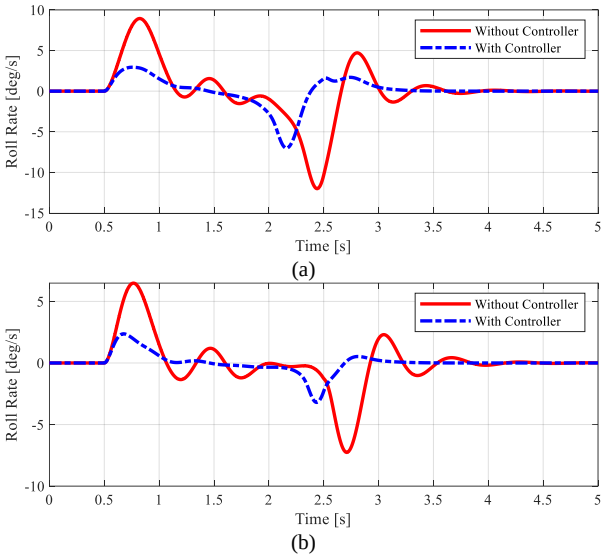

Figs. 20. Roll rate of vehicle for (a) μ = 0.9 (b) μ = 0.5

The percentage of reduction for roll angle is 60.4% and 60.4% for μ = 0.9 and 0.5, respectively. The maximum absolute values of roll rate without and with controller are 12.00 and 7.02 deg, respectively for μ = 0.9. With μ = 0.5, the maximum absolute values of roll rate without and with controller are 7.26 and 3.20 deg, respectively. The percentages of reduction in roll rate are 41.5% and 55.9% for μ = 0.9 and 0.5, respectively. The controller can also reduce maximum absolute value of the pitch angle and pitch rate of the vehicle as shown in Figs. 21(a) and (b) and Figs. 22(a) and (b) for μ = 0.9 and 0.5. The maximum absolute values of the pitch angle without and with controller for μ = 0.9 are 0.28 and 0.17 deg, respectively while the maximum absolute values of pitch angle without and with controller for μ = 0.5 are 0.28 and 0.16 deg, respectively.

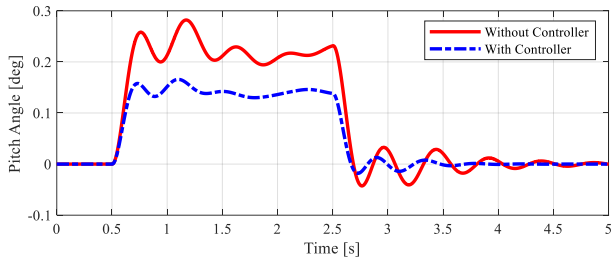

(a)

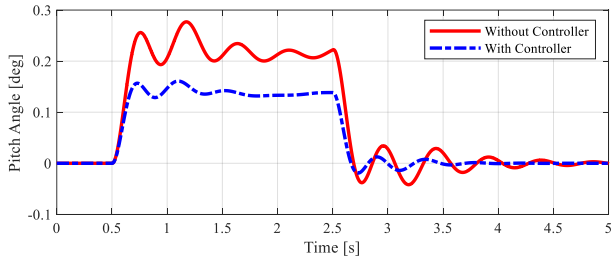

(b)

Figs. 21. Pitch angle of vehicle for (a) μ = 0.9 (b) μ = 0.5

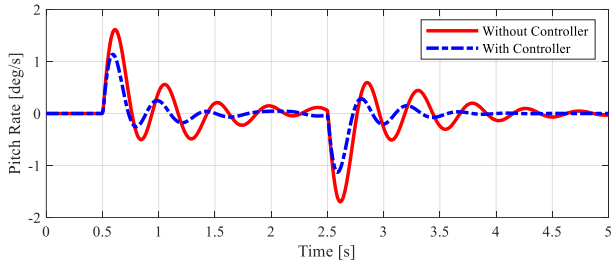

(a)

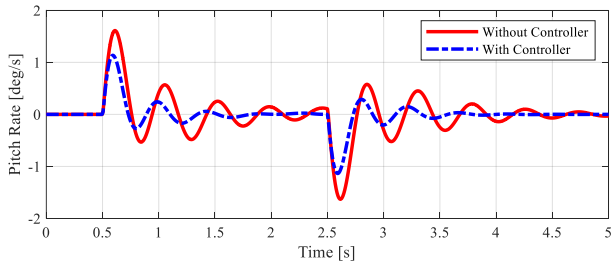

(b)

Figs. 22. Pitch rate of vehicle for (a) μ = 0.9 (b) μ = 0.5

The percentages of reduction for pitch angle for μ = 0.9 and 0.5 are 41.2% and 41.9%, respectively. The maximum absolute values of pitch rate without and with controller are 1.70 and 1.14 deg, respectively for μ = 0.9. With μ = 0.5, the maximum absolute values of pitch rate without and with controller are 1.63 and 1.14 deg, respectively.

The percentages of reduction in pitch rate are 33.0% and 30.4% for μ = 0.9 and 0.5, respectively.

V. Conclusion

In this study, a 10-degree-of-freedom vehicle model with Dugoff's tire model is used to simulate the vehicle behavior. The vehicle is validated by comparing the results with the model in CarSim by using the double lane change and step steering input tests, in which the results have showed that the vehicle model used in this study can emulate the vehicle model in CarSim.

Proportional-derivative controllers with the addition of the products of acceleration and gain were proposed to calculate the desired vertical vehicle forces, roll moment, and pitch moment to mitigate the vertical, roll, and pitch motions of the vehicle. These forces are converted into active suspension forces using decoupling transformation.

The performance of the controllers is evaluated by giving single sine steer wave and braking torque inputs to the vehicle. The vertical, roll, and pitch motions of the vehicle are compared to the case without controllers. The results have showed that the controllers successfully reduce the vertical, roll, and pitch motions. This study could be further improvised by including the models for hydraulic actuator or magnetorheological damper to obtain results that are more realistic. Future study could also focus on the design of the combined control of active suspension, active steering, and active braking in an emergency lane change scenario and the effect of this combined control on vehicle dynamics performance can be investigated.

Acknowledgements

This research is supported by a grant from the Ministry of Higher Education Malaysia with a grant number FRGS/1/2020/TK0/UTEM/02/38. The authors would like to acknowledge support from Universiti Teknikal Malaysia Melaka for providing the research facilities.

References

[1] Phuman Singh, A., Abu Kassim, K., Koetniyom, S., Ubaidillah, U., Lane Change Aspect Ratio and Dimensionless Path for Emergency Obstacle Avoidance, (2022) *International Review of Mechanical Engineering (IREME)*, 16 (4), pp. 198-205. doi:https://doi.org/10.15866/ireme.v16i4.22083

[2] Phuman Singh, A., Hui, L., Abu Kassim, K., Koetniyom, S., Emergency Lane Change with a Vehicle in the Neighbouring Lane, (2022) *International Review of Mechanical Engineering (IREME)*, 16 (5), pp. 214-221. doi:https://doi.org/10.15866/ireme.v16i5.22169

[3] J. Ackermann and D. Odenthal, Robust steering control for active rollover avoidance of vehicles with elevated center of gravity,

Proceedings AVCS'98, 1998, pp. 118–123.
[4] J. Yoon, W. Cho, B. Koo, and K. Yi, Unified chassis control for rollover prevention and lateral stability, *IEEE Transactions on Vehicular Technology*, vol. 58, no. 2, pp. 596–609, 2009. doi: 10.1109/TVT.2008.927724
[5] J. Yoon, S. Yim, W. Cho, B. Koo, and K. Yi, Design of an unified chassis controller for rollover prevention, manoeuvrability and lateral stability, *Vehicle System Dynamics*, vol. 48, no. 11, pp. 1247–1268, 2010. doi: 10.1080/00423110903536403
[6] F. Jia, H. Jing, Z. Liu, and M. Gu, Cooperative control of yaw and roll motion for in-wheel motor vehicle with semi-active suspension, *Proceedings of the Institution of Mechanical Engineers, Part D: Journal of Automobile Engineering*, vol. 236, no. 1, pp. 3–15, 2022. doi: 10.1177/09544070211020827
[7] W. Cho, J. Suh, and S.-H. You, Integrated Motion Control Using a Semi-Active Damper System to Improve Yaw-Roll-Pitch Motion of a Vehicle, *IEEE Access*, vol. 9, pp. 52464–52473, 2021. doi: 10.1109/ACCESS.2021.3070366
[8] G. Savaia, M. Corno, G. Panzani, A. Sinigaglia, and S. M. Savaresi, Pitch Control for Semi-Active Suspensions: Open-loop and Closed-loop Strategies, 2021 *IEEE Conference on Control Technology and Applications (CCTA)*, Aug. 2021, pp. 14–19. doi: 10.1109/CCTA48906.2021.9658884
[9] A. S. P. Singh and I. Z. M. Darus, Active Roll Control Strategy Using Fuzzy Logic Control Active Suspension, *WSEAS Transactions on Systems and Control*, vol. 9, no. 1, pp. 566–573, 2014.
[10] Z. A. Kadir, K. Hudha, H. Jamaluddin, F. Ahmad, and F. Imaduddin, Active roll control suspension system for improving dynamics performance of passenger vehicle, *Proceedings of 2011 International Conference on Modelling, Identification and Control, ICMIC* 2011, 2011, pp. 492–497. doi: 10.1109/icmic.2011.5973755
[11] S. Liu, T. Zheng, D. Zhao, R. Hao, and M. Yang, Strongly Perturbed Sliding Mode Adaptive Control Of Vehicle Active Suspension System Considering Actuator Nonlinearity, *Vehicle System Dynamics*, vol. 60, no. 2, pp. 597–616, Feb. 2022. doi: 10.1080/00423114.2020.1840598
[12] F. Ahmad, K. Hudha, F. Imaduddin, and H. Jamaluddin, Modelling, Validation And Adaptive PID Control With Pitch Moment Rejection Of Active Suspension System For Reducing Unwanted Vehicle Motion In Longitudinal Direction, *International Journal of Vehicle Systems Modelling and Testing*, vol. 5, no. 4, pp. 312–346, 2010.
[13] V. T. Vu, O. Sename, L. Dugard, and P. Gaspar, Enhancing Roll Stability Of Heavy Vehicle By LQR Active Anti-Roll Bar Control Using Electronic Servo-Valve Hydraulic Actuators, *Vehicle System Dynamics*, vol. 55, no. 9, pp. 1405–1429, 2017. doi: 10.1080/00423114.2017.1317822
[14] S. Sato and H. Fujimoto, Proposal of pitching control method based on slip-ratio control for electric vehicle, *IECON Proceedings (Industrial Electronics Conference)*, pp. 2823–2828, 2008. doi: 10.1109/IECON.2008.4758406
[15] D. Tavernini, E. Velenis, and S. Longo, Feedback Brake Distribution Control For Minimum Pitch, *Vehicle System Dynamics*, vol. 55, no. 6, pp. 902–923, 2017. doi: 10.1080/00423114.2017.1293275
[16] S. Yim, K. Jeon, and K. Yi, An Investigation Into Vehicle Rollover Prevention By Coordinated Control Of Active Anti-Roll Bar And Electronic Stability Program, *International Journal of Control, Automation and Systems*, vol. 10, no. 2, pp. 275–287, 2012. doi: 10.1007/s12555-012-0208-9
[17] B. C. Chen and H. Peng, Differential-Braking-Based Rollover Prevention For Sport Utility Vehicles With Human-In-The-Loop Evaluations, *Vehicle System Dynamics*, vol. 36, no. 4–5, pp. 359–389, 2001. doi: 10.1076/vesd.36.4.359.3546
[18] N. Yoshikawa, A. Kato, P. Raksincharoensak, H. Okamoto, K. Oshima, and T. Sonehara, Study on Enhancing Rollover Resistance of Micro-Scale Electric Vehicle by Using Direct Yaw-Moment Control, *Transactions of Society of Automotive Engineers of Japan*, vol. 48, no. 2, pp. 363–369, 2017. doi: 10.11351/jsaeronbun.48.363
[19] E. Katsuyama, Decoupled 3D Moment Control Using In-Wheel Motors, *Vehicle System Dynamics*, vol. 51, no. 1, pp. 18–31, 2013. doi: 10.1080/00423114.2012.708758
[20] S. Solmaz, M. Corless, and R. Shorten, A Methodology For The Design Of Robust Rollover Prevention Controllers For Automotive Vehicles With Active Steering, *International Journal of Control*, vol. 80, no. 11, pp. 1763–1779, 2007. doi: 10.1080/00207170701473987
[21] Y. Zhang, A. Khajepour, and X. Xie, Rollover prevention for sport utility vehicles using a pulsed active rear-steering strategy, *Proceedings of the Institution of Mechanical Engineers, Part D: Journal of Automobile Engineering*, 2016, vol. 230, no. 9, pp. 1239–1253. doi: 10.1177/0954407015605696
[22] T. Shim and D. Toomey, Investigation Of Active Steering/Wheel Torque Control At The Rollover Limit Maneuver, *SAE Technical Papers*, no. 724, 2004. doi: 10.4271/2004-01-2097
[23] T. Shim, D. Toomey, C. Ghike, and H. M. Sardar, Vehicle Rollover Recovery Using Active Steering/Wheel Torque Control, *International Journal of Vehicle Design*, vol. 46, no. 1, pp. 51–71, 2008. doi: 10.1504/IJVD.2008.017069
[24] B. Mashadi, M. Mokhtari-Alehashem, and H. Mostaghimi, Active vehicle rollover control using a gyroscopic device, *Proceedings of the Institution of Mechanical Engineers, Part D: Journal of Automobile Engineering*, 2016, vol. 230, no. 14, pp. 1958–1971. doi: 10.1177/0954407016641322
[25] N. Ochi, H. Fujimoto, and Y. Hori, Proposal of roll angle control method using positive and negative anti-dive force for electric vehicle with four in-wheel motors, 2013 *IEEE International Conference on Mechatronics, ICM* 2013, 2013, pp. 816–821. doi: 10.1109/ICMECH.2013.6519146
[26] R. Rajamani, *Vehicle Dynamics and Control*, (2nd edition. New York: Springer, 2012).
[27] S. Ikenaga, F. L. Lewis, J. Campos, and L. Davis, Active suspension control of ground vehicle based on a full-vehicle model, *Proceedings of the 2000 American Control Conference. ACC (IEEE Cat. No.00CH36334)*, 2000, vol. 6, no. June, pp. 4019–4024 vol.6. doi: 10.1109/ACC.2000.876977
[28] Bataineh, A., Batayneh, W., Okour, M., Intelligent Control Strategies for Three Degree of Freedom Active Suspension System, (2021) *International Review of Automatic Control (IREACO)*, 14 (1), pp. 17-27. doi:https://doi.org/10.15866/ireaco.v14i1.20057
[29] Mazrekaj, R., Lajqi, S., Mema, F., Lajqi, N., The Influence of the Vehicle Shock Absorber Wearing on the Performance of the Braking System – A Case Study, (2021) *International Journal on Engineering Applications (IREA)*, 9 (3), pp. 137-147. doi:https://doi.org/10.15866/irea.v9i3.20493
[30] Reddipogu, J., Elumalai, V., Multi-Objective Model Predictive Control for Vehicle Active Suspension System, (2020) *International Review of Automatic Control (IREACO)*, 13 (5), pp. 255-263. doi:https://doi.org/10.15866/ireaco.v13i5.19212
[31] Calì, M., Oliveri, S., Design of Active Tyre-Suspension-Seat System Through Multibody Model and Genetic Algorithms, (2021) *International Review on Modelling and Simulations (IREMOS)*, 14 (6), pp. 496-503. doi:https://doi.org/10.15866/iremos.v14i6.21627

Authors' information

[1]Fakulti Kejuruteraan Mekanikal, Universiti Teknikal Malaysia Melaka, Hang Tuah Jaya, 76100 Durian Tunggal, Melaka, Malaysia.

[2]Centre for Advanced Research on Energy, Universiti Teknikal Malaysia Melaka, Hang Tuah Jaya, 76100 Durian Tunggal, Melaka, Malaysia.

[3]Malaysian Institute of Road Safety Research, 125-135, Jalan TKS 1, Taman Kajang Sentral, 43000 Kajang, Selangor, Malaysia.

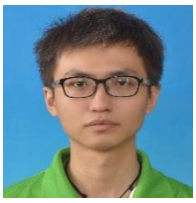

Adam Puah Leong Zhin received the B. Eng. degree in Mechanical Engineering from Universiti Teknikal Malaysia Melaka, Melaka, Malaysia, in 2020.
He is currently a Mechanical Engineering master's degree student with the Fakulti Kejuruteraan Mekanikal, Universiti Teknikal Malaysia Melaka. His current research interests include collision avoidance and integrated chassis control.

Amrik Singh Phuman Singh received the B. Eng. degree in Mechanical Engineering from Universiti Teknikal Malaysia Melaka, Melaka, Malaysia, in 2009, the M. Eng. degree in Mechanical Engineering from Universiti Teknologi Malaysia, Johor, Malaysia, in 2012, and the Ph.D. degree in Vehicle Control Systems from the Department of Systems Science, Kyoto University, Kyoto, Japan, in 2019.
He is currently a Senior Lecturer with the Fakulti Kejuruteraan Mekanikal, Universiti Teknikal Malaysia Melaka. His current research interests include collision avoidance and integrated chassis control.

Khairil Anwar Abu Kassim received the B. Eng. degree in Mechanical Engineering from Okayama University of Science, Okayama, Japan, in 2000, the master's degree in Engineering management from Universiti Putra Malaysia, Selangor, Malaysia, in 2008, and the Ph.D. degree in Business Administration from the UCSI University, Kuala Lumpur, Malaysia, in 2017.
He is currently the Director General of the Malaysian Institute of Road Safety and the Secretary General of ASEAN NCAP. His current research interests include passive and active vehicle safety systems. Dr. Khairil is the Editor-In-Chief for the Journal of the Society of Automotive Engineers Malaysia and the International Journal of Road Safety.

Fauzi Ahmad received the B. Eng. degree in Mechanical Engineering and M. Sc. Degree in Mechanical Engineering from Universiti Teknikal Malaysia Melaka, Melaka, Malaysia, in 2007, and 2010, respectively, and the Ph.D. degree in Vehicle Dynamic and Control from the from the Universiti Teknologi Malaysia in 2017.
He is currently a Senior Lecturer with the Fakulti Kejuruteraan Mekanikal, Universiti Teknikal Malaysia Melaka. His current research interests include include vehicle control, X-by-wire system and electric vehicles.

Mohd Azman Abdullah received the B. Sc. degree in Mechanical Engineering from Universiti Tenaga Nasional, Malaysia, in 2002, the M. Sc. degree in Automotive and Motorsport Engineering from Brunel University, UK, in 2005, and the Ph.D. degree in Mechanical Control Systems from the Tokyo University of Agriculture and Technology, Japan in 2011.
He is currently an Associate Professor with the Fakulti Kejuruteraan Mekanikal, Universiti Teknikal Malaysia Melaka. His current research interests include include vehicle dynamics, vehicle control systems, and railway vehicle mechanisms.